Iranian Journal of Oil & Gas Science and Technology, Vol. 4 (2015), No. 1, pp. 01-16
http://ijogst.put.ac.ir

Removal of Sulfur and Nitrogen Compounds from Diesel Fuel Using MSU-S

Sina Rashidi[1], Mohammad Reza Khosravi Nikou[2*], Bagher Anvaripour[1], and Touba Hamoule[2]

[1] Department of Chemical Engineering (HSE), Petroleum University of Technology, Abadan, Iran
[2] Department of Gas Engineering, Petroleum University of Technology, Ahwaz, Iran

Received: October 30, 2014*; revised:* December 09, 2014*; accepted:* December 22, 2014

Abstract

The performance of MSU-S and its forms modified with phosphotungstic acid (HPW) and nickel (Ni) for the desulfurization and denitrogenation of model diesel fuel were studied. According to the results of the characteristic tests (N_2 adsorption-desorption, XRD, SEM, and NH_3-TPD), heteropoly acid incorporation causes higher acidity along with a negligible loss of structural aspects, while Ni impregnation leaves a drastic negative effect on mesoporous structure, crystalline phase, and particle shape along with a positive impact on surface acidity. With both modifications (HPW and Ni), the maximum increase of 33.18% and 6.88% was occurred for the adsorption loading of total sulfur and total nitrogen respectively. The adsorption loading and selectivity of all the adsorbents for total nitrogen were slightly more than those for total sulfur (the selective adsorption of nitrogen over sulfur). The pseudo-second order model can best fit the kinetics data and Freundlich model can best describe the equilibrium isotherm for all the species over Ni/HPW-MSU-S.

Keywords: Desulfurization, Denitrogenation, MSU-S, HPW, Nickel

1. Introduction

Fuels containing sulfur and nitrogen impurities in internal combustion engines will be resulted in SO_x and NO_x emissions, which, during combustion processes, not only have an inhibiting effect on catalysts in catalytic converters, but also result in an acid rain and the other air pollutions (Kim et al., 2006; Erisman et al., 2007; Dehkordi et al., 2009; Wen et al., 2010; Sarda et al., 2012; Arcibar-Orozco et al., 2013; Shahadat Hussain et al., 2013; Xu et al., 2014). Moreover, sulfur and nitrogen compounds, predominantly H_2S and NH_3, produced during the catalytic reforming of fuels, can poison the precious metal electrodes and catalysts in fuel cells, resulting in an adverse effect on the quality of petroleum products (Kim et al., 2006; Chen et al., 2009; Dehkordi et al., 2009; Wen et al., 2010; Wang et al., 2012; Shahadat Hussain et al., 2013; Xu et al., 2013; Xu et al., 2014). These compounds also have health hazards through affecting various organs and systems such as respiratory damages, cardiovascular diseases, lung cancer, etc. (Kraft et al., 2005; Bernstein et al., 2008; Kampa et al., 2008; Latza et al., 2009; Pan, 2011). Due to the health and environmental hazards as well as the applicability of catalytic processes, only fuels with ultra-low levels of sulfur and nitrogen content will be allowable in highway consumptions, and particularly, fuel cell systems in the near future (Kim et al., 2006; Dehkordi et al., 2009; Wen et al., 2010; Sarda et al., 2012; Shahadat Hussain et al., 2013;

* Corresponding Author:
Email: mr.khosravi@put.ac.ir

Xu et al., 2014). Therefore, desulfurization and denitrogenation are necessary for the utilization of liquid fuels as ultra-clean automotive fuels for transportation applications and as hydrogen sources for on-board applications (Kim et al., 2006; Wen et al., 2010). Because of difficulty, complication, the requirement of large sizes in reactors, valving, actuators, and associated equipment, high operational temperatures (300–400 °C) and pressures (3–6 MPa), and high hydrogen consumption, hydrodesulfurization (HDS) and hydrodenitrogenation (HDN) have low efficiency in producing ultra-clean fuels (Chen et al., 2009; Dehkordi et al., 2009; Wen et al., 2010; Wang et al., 2012; Shahadat Hussain et al., 2013; Xu et al., 2013; Yang et al., 2013). Oxidative desulfurization (ODS) and oxidative denitrogenation (ODN), carried out in the liquid phase and under very mild operating conditions, have been overshadowed because of cost and applicability factors due to consuming oxidizing agents and catalysts (Dehkordi et al., 2009). Using adsorbents under ambient conditions for selective removing of sulfur and/or nitrogen compounds in liquid hydrocarbon fuels has been attracted much interest; because it is a inexpensive, simple, applicable, and environmentally friendly process useful for a lot of applications such as fuel cells (Kim et al., 2006; Chen et al., 2009; Dehkordi et al., 2009; Koriakin et al., 2010; Sun et al., 2010; Wen et al., 2010; Arcibar-Orozco et al., 2013; Shahadat Hussain et al., 2013; Xu et al., 2014). Several materials such as zeolite-based materials, silica-based materials, activated carbons, metal oxides, metal sulfides (supported base on transition metals), and silica gel have been reported as adsorbents for the selective removal of sulfur and nitrogen containing compounds from liquid hydrocarbon fuels at ambient temperature and pressure (Kim et al., 2006; Koriakin et al., 2010; Meng et al., 2010; Wen et al., 2010; Santos et al., 2012; Sarda et al., 2012; Wang et al., 2012; Xu et al., 2013, 2014). In 2010, Meng et al. worked on the desulfurization of a model gasoline (600 ppmw thiophene or DBT in n-octane) by selective adsorption over Ag^+ exchanged Al-MSU-S through a fixed bed; the best adsorbent, i.e. Ag^+/20%Al-MSU-S, had an adsorption capacity (model gasoline/adsorbent) of 5 ml/g and 20 ml/g for thiophene and DBT respectively. Santos et al. (2012) reported that the incorporation of the molybdenum oxide into a commercial silica–alumina-based adsorbent would be promising for S/N removal from a commercial hydrotreated Brazilian diesel if the loss in surface area is better controlled. An investigation was done on the performance of Ag/TiO_x-Al_2O_3 and Ag/TiO_x-SiO_2 for desulfurizing different fuels; finally, 4% Ag/TiO_x-Al_2O_3 demonstrated saturation capacities of 10.11, 6.11, 7.4, and 0.59 mg S/(gram adsorbent) for JP5, JP8, ORD, and ULSD respectively (Shahadat Hussain et al., 2013). Xu et al. attained the adsorption capacity of 0.633 mg S/(g A) (at a breakthrough sulfur concentration of 10 ppmw) by using a novel low-cost hybrid mesoporous material, i.e. $10NiO$-$CeO_2/7.5Al_2O_3$-SiO_2, for selectively removing sulfur from real Jet-A fuel (1037 ppmw of S) in fixed-bed tests (Xu et al., 2014). In the present work, a silica–alumina-based adsorbent modified with a heteropoly acid and loaded with nickel oxide has been studied for the desulfurization and denitrogenation of a model diesel fuel.

2. Experimental procedure

2.1. Chemicals

Cab-O-sil M-5, sodium aluminate and phosphotungstic acid (HPW) were purchased from Sigma-Aldrich Chemical Co. (USA). Toluene, naphthalene, n-octane, n-hexadecane, quinoline, carbazole, thiophene, dibenzothiophene, tetrapropylammonium hydroxide (TPAOH 40% aqueous solution), hexadecyltrimethylammonium bromide (HTABr) and nickel (II) nitrate hexahydrate were purchased from Merck Co. (Germany). All the materials were used as received without further purification. Deionized water was employed in the experiments.

2.2. Synthesis

a. MSU-S

Mesoporous MSU-S (MFI) was synthesized through the procedure described by Liu et al. (Liu et al., 2001). 10.2 g of TPAOH as an MFI structure director was added to 79.26 g of deionized water. Then, 0.34 g of sodium aluminate and 6.0 g of Cab-O-sil M-5, as the aluminum and silicon sources respectively, were added to the solution of water and TPAOH. The final mixture was kept under stirring in a flask at 50 °C for 18 hrs (zeolite MFI seeds were formed). Then, 100 g of deionized water and 9.44 g of HTABr as the surfactant were mixed and introduced to the seeds suspension to assemble a mesoporous structure. Lastly, pH was adjusted at 9 by adding sulfuric acid. The final gel was introduced to a Teflon-lined stainless steel autoclave and placed into the oven (MEMERT) at 150 °C for 48 hrs. The product was washed with deionized water, filtered, and dried at 80 °C for 10 hrs. Then, the white product was ion exchanged with a solution of 0.1 M NH_4NO_3 in 96% ethanol at the reflux temperature for 2 hrs. Afterwards, the product was dried at 90 °C for 12 hrs, and finally calcined at 550 °C in air for 10 hrs in a muffle furnace (SHIN SAENG, SEF-201P) at a heating rate of 1 °C/min.

b. HPW-MSU-S

A direct synthesis method for the better dispersion of HPW in the MSU-S structure was utilized (Gagea et al., 2009). 10% HPW-MSU-S was prepared according to the following procedure.

10 wt.% HPW and 100 g of water were mixed and kept under stirring for 24 hrs (Solution 1). After 6 hr, 10.2 g of TPAOH, 79.26 g of deionized water, 0.34 g of sodium aluminate, and 6.0 g of Cab-O-sil M-5 were mixed and kept under stirring at 50 °C for 18 hrs (Solution 2). Afterwards, 9.44 g of HTABr was mixed with Solution 2. Then, Solution 2 was well mixed with Solution 1 and pH was set at 9. Next, the gel was subjected to heating, washing, filtering, drying, ion exchanging, again drying, and finally calcination in the same manner as MSU-S.

c. Modification

For preparing 10 wt.% metal loaded supports, the required amount of metal precursor ($Ni(NO_3)_2 \cdot 6H_2O$) was dissolved in deionized water and then added to a certain amount of adsorbent while stirring at 40 °C for moisture evaporation; it was next dried at 90 °C for 12 hrs in oven and finally calcined at 550 °C for 4 hrs using a muffle furnace at a heating rate of 1 °C/min (Santos et al., 2012; Sarda et al., 2012).

2.3. Characterization

The X-ray diffraction (XRD) analysis was performed by using an X-PERT diffractometer, which was equipped with an Ni filter, used Cu kα radiation, and operated at 40 kV and 40 mA (2θ range of 0-10° for MSU-S and 0-80° for HPW-MSU-S and Ni/HPW-MSU-S). Specific surface area (BET), total pore volume, average pore size diameter, and distribution (BJH) were determined by N_2 adsorption-desorption isotherms at -196 °C obtained from a NOVA 2200 instrument (Quantachrome, USA). Prior to the analysis, all the samples were degassed under a flow of N_2 at 350 °C for 6 hrs. A PulseChemiSorb 2705 instrument (Micromeritics, USA) with a conventional flow apparatus, and the on-line thermal conductivity detection (TCD) was employed to measure the acidity of the adsorbents via NH_3-TPD by heating at a rate of 10 °C/min, under a flow of helium carrier gas (30 ml/min), from 30 °C to 500 °C. The amount of effluent ammonia was then measured using TCD and recorded as a

function of temperature. Determining the morphology of the synthesized materials was carried out using scanning electron microscopy (SEM); the samples were treated by gold before imaging.

2.4. Model fuel

Eight compounds were chosen for making the model fuel most similar to real fuel and then three types of the model fuels, namely sulfur-nitrogen rich fuel, sulfur rich fuel, and nitrogen rich fuel were considered. The composition of all the model fuels is listed in Table 1.

Table 1
The concentration of each compound in the model fuels.

Chemicals	Concentration					
	Model Fuel #1 (S & N containing Diesel)		Model Fuel #2 (nitrogen-free Diesel)		Model Fuel #3 (sulfur-free Diesel)	
	wt.%	ppmw of S or N	wt.%	ppmw of S	wt.%	ppmw of N
Sulfur compounds						
Thiophene	0.23	876.51	0.22	838.40	---	---
DBT	0.21	365.46	0.22	382.86	---	---
Nitrogen compounds						
Carbazole	0.13	108.90	---	---	0.14	117.28
Quinoline	0.15	162.67	---	---	0.14	151.82
Aromatics						
Naphthalene	4.00	---	4.00	---	4.00	---
Toluene	7.00	---	7.00	---	7.00	---
Paraffins						
n-Hexadecane	44.14	---	44.28	---	44.36	---
n-Octane	44.14	---	44.28	---	44.36	---

2.5. Adsorption test procedure

For each test run, 5 g of the model fuel with 0.1 g of the adsorbent was mixed in a flask while being agitated at a constant rate of 200 rpm at room temperature for 24 hrs. Afterwards, the residual concentration of sulfur and nitrogen elements or compounds was measured.

2.6. Analysis of fuel

Measuring the total sulfur and total nitrogen concentrations was carried out by an analytical Jena E3400 TS/TN analyzer. To determine the compound concentration, fuel samples were analyzed by an Agilent 6890 gas chromatograph equipped with a capillary column (HP-5, L: 30m, ID: 0.32mm, DF: 0.25µm; Restek Corp.) and a flame ionized detector (FID). Both TS/TN analyzer and gas chromatograph were calibrated using the standard samples of the model fuels. The adsorption efficiency (η), total adsorption loading in a mass basis (q), and total adsorption capacity per specific area (Q) were calculated as follows:

Adsorption efficiency:

$$(\eta_i(\%)) = (C_{0i} - C_{si}/C_{0i}) \times 100 \quad (1)$$

Adsorption loading:

$$(q_i(mmol/g)) = (m_{fuel}(C_{0i} - C_{si}))/(m_{ads} \times Mw_i) \quad (2)$$

Adsorption capacity:

$$(Q_i(mg/m^2)) = (q_i/S_{BET}) \times Mw_i \quad (3)$$

Sulfur selectivity = $q_S/(q_S + q_N)$ (4)

where, C_{0i}, C_{si}, m_{fuel}, and m_{ads} are the compound initial concentration (ppmw), the compound residual concentration (ppmw), the mass of fuel sample (kg), and the mass of the adsorbent (g) respectively. S_{BET} is the specific surface area of the adsorbent ($m^2 \cdot g^{-1}$) and Mw_i represent the molecular/atomic weight of the compound/element ($g.mol^{-1}$).

3. Results and discussion

3.1. Adsorbent properties

a. XRD spectra

The low-angle XRD pattern of MSU-S and the total-angle patterns of HPW-MSU-S and Ni/HPW-MSU-S adsorbents are shown in Figure 1. A distinct diffraction peak is illustrated in the inset of Figure 1, which is the characteristic of the hexagonal mesostructure in MSU-S (Lourenço et al., 2006; Meng et al., 2010; Wang et al., 2010). The high-angle region of the synthesized HPW-MSU-S does not show the characteristic diffraction pattern of crystalline HPW phase, which is an evidence of the high dispersion of HPW in the structure of MSU-S. Furthermore, by considering the peak with the almost same intensity as that of MSU-S, it can be concluded that the mentioned method for the synthesis of HPW-MSU-S is an appropriate way for the incorporation of heteropoly acid into the MSU-S support with a limited destructive effect on its structure. In the total-angle XRD pattern of Ni/HPW-MSU-S, in addition to the peak of hexagonal mesostructure for MSU-S, there are four peaks in the high-angle region, one of smooth type and three of sharp one. All the four peaks confirm the formation of NiO crystalline phase over the HPW-MSU-S after the surface modification (Santos et al., 2012). In this case, the peak intensity of MSU-S obviously decreases with impregnating the nickel species, representing the relative conversion of crystalline phase to amorphous type. Thus the surface loading of nickel by dry impregnation has an adverse effect in mesoporous template of MSU-S.

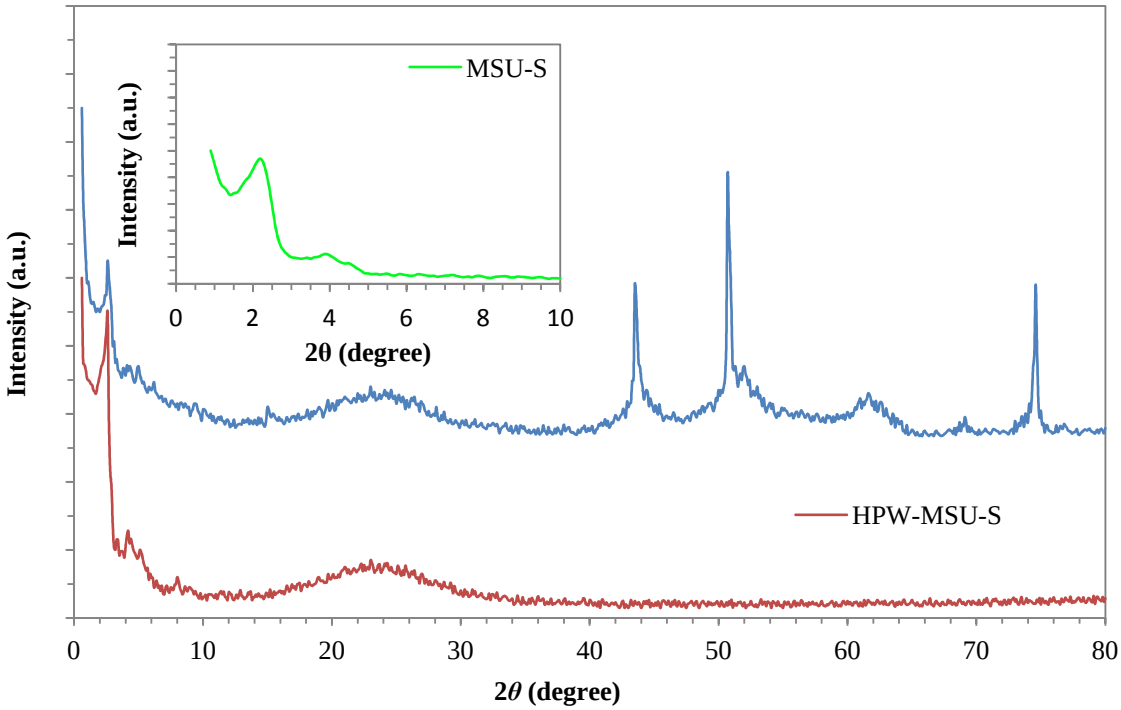

Figure 1
XRD pattern of the three adsorbents.

b. N_2 adsorption-desorption data

According to the BET results, it is found that there is no significant difference between the specific surface area of HPW-MSU-S and MSU-S (649.2 and 678.5 m^2/g respectively); however, a slight difference in average pore diameter and total pore volume of the two adsorbents is seen, which shows the perfect dispersion of HPW molecules in the structure of MSU-S (in line with the XRD results). On the other hand, Ni/HPW-MSU-S has a low surface area (351.3 m^2/g) compared to the other adsorbents, for which the pore blockage of the adsorbent by nickel particles is the most probable cause. Both average pore diameter and total pore volume of Ni/HPW-MSU-S (24.47 Å and 0.68 cm^3/g respectively) are surprisingly more than those of HPW-MSU-S (23.21 Å and 0.58 cm^3/g respectively) and those of MSU-S (24.39 Å and 0.65 cm^3/g respectively). It may be due to the destruction of mesopore structure by Ni species, leading to the creation of the macropores, which can obviously be seen in the pore size distribution of the adsorbent (see Figure 3). The nitrogen adsorption-desorption isotherms for all the three adsorbents are shown in Figure 2. All of them show the classical shape of the type IV isotherm, typical for mesoporous materials with a uniform and narrow pore distribution (Sing, 1985; Rouquerol et al., 1994; Lourenço et al., 2006; Meng et al., 2010; Naik et al., 2010), Moreover, the narrow Gaussian pore size distributions in Figure 3 suggests that the samples possess very regular mesoporous channels (except for Ni/HPW-MSU-S with a little irregularity due to the macroporosity).

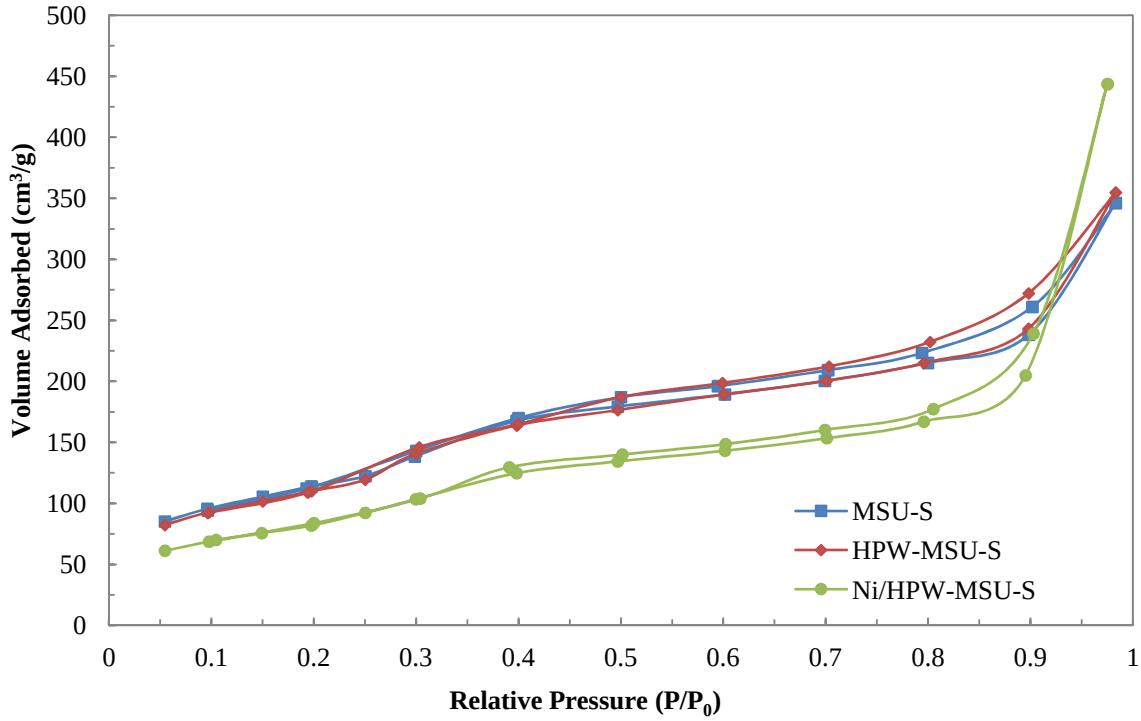

Figure 2
N_2 adsorption-desorption isotherm for the three adsorbents.

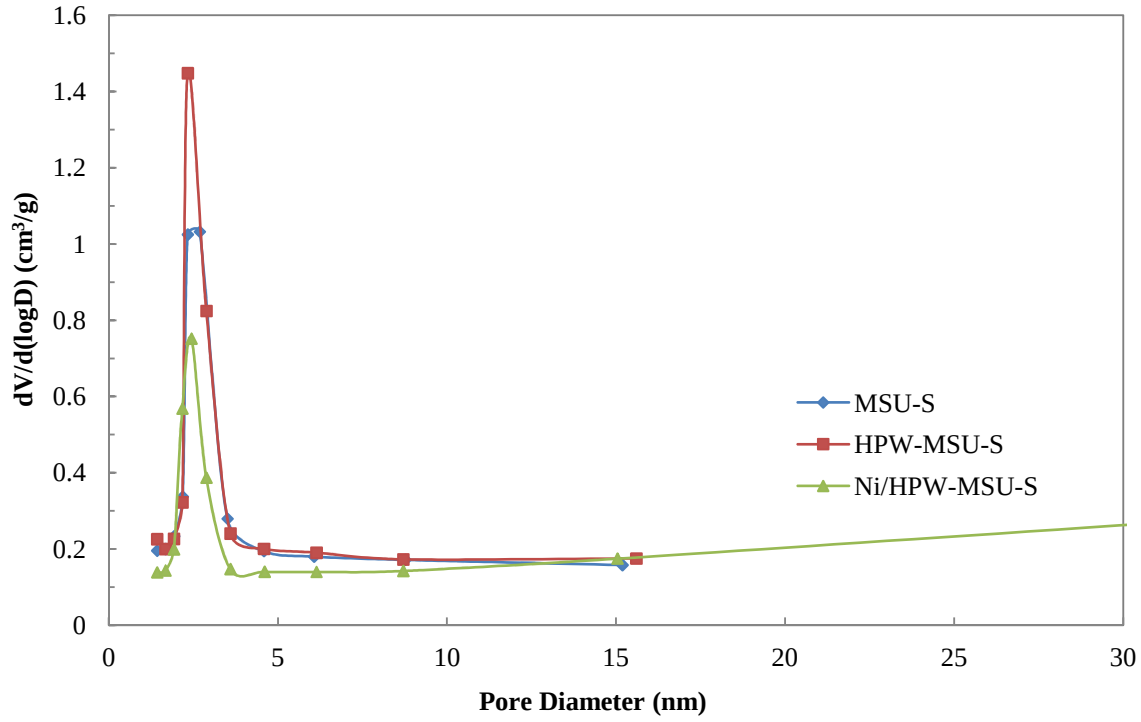

Figure 3
Pore size distribution of the three adsorbents.

c. NH_3-TPD spectra

The NH_3-TPD spectra of MSU-S, HPW-MSU-S, and Ni/HPW-MSU-S are shown in Figure 4. The amount of ammonia desorbed from the Ni/HPW-MSU-S (0.714 mmol/g) is much more than those from HPW-MSU-S and MSU-S (0.386 and 0.271 mmol/g respectively); this is verified by Figure 4 in which the area under desorption profiles of Ni/HPW-MSU-S is greater than the two others. This indicates the most acid content in Ni-modified adsorbent. Only the first three peaks in NH_3-TPD profile of Ni/HPW-MSU-S have to be taken into account for investigating the acidity of adsorbent, because the sorption temperature of two last peaks is higher than the temperature considered for the calcination of the adsorbent, meaning that the structure of the support is extremely damaged and thus the following acidities are not valid in case of MSU-S. Furthermore, the maximum desorption temperature of NH_3 for Ni/HPW-MSU-S (493 °C) is the highest value compared to those for HPW-MSU-S and MSU-S (210 and 206 °C respectively), denoting the strongest acid sites in nickel-incorporated MSU-S. The multi-peak profile of Ni/HPW-MSU-S is arising from the presence of various acid sites with different strengths. For HPW-MSU-S and MSU-S, only a single peak is seen, which is leading to the presence of one type of acidity (Kugita et al., 2003; Gagea et al., 2009). Hence it is concluded that Ni/HPW-MSU-S has the most acidic sites with the highest acidity strength, and, between the two other adsorbents, HPW-MSU-S outperforms MSU-S from an acidity point of view.

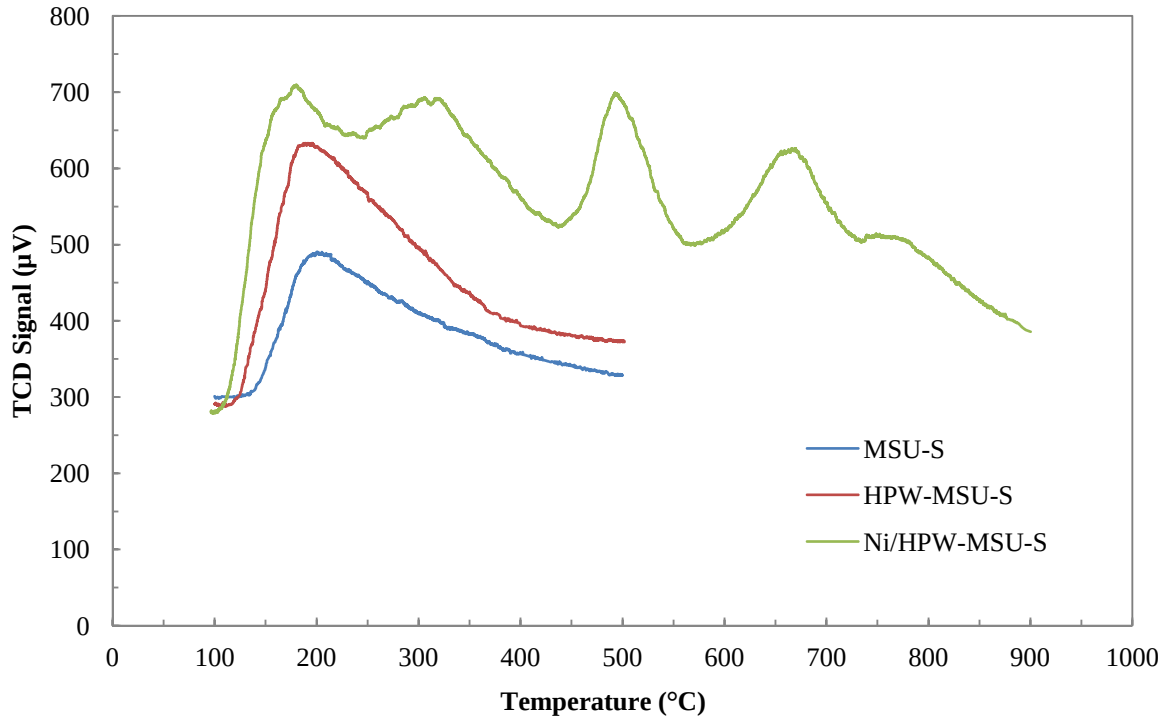

Figure 4
NH_3-TPD profile of the three adsorbents.

d. SEM images

SEM images of all the prepared samples are displayed in Figure 5 on a 1 µm scale. The MSU-S and HPW-MSU-S samples show aggregates of rounded particles (part (a) and (b) respectively), as opposed to the irregular shapes for Ni/HPW-MSU-S (part (c)). The particle size of the sample modified with both heteropoly acid and nickel is generally much bigger than that of the adsorbents

without Ni loading. Hence it can be guessed that the nickel particles attached the MSU-S parts to each other or were not dispersed appropriately over the surface of MSU-S (Ni agglomeration).

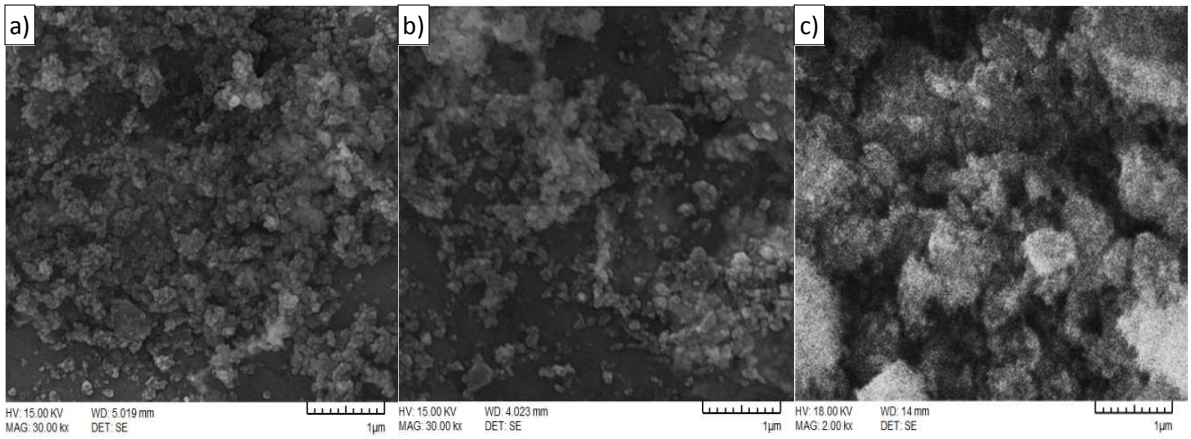

Figure 5
SEM image of MSU-S (a), HPW-MSU-S (b), and Ni/HPW-MSU-S (c).

3.2. Adsorption study

The results of the adsorption tests using 0.1 g of adsorbent and 5 g of fuel are shown in Table 2 (MSU-S is summarized as MSU). The adsorptive loadings of nitrogen obviously are higher than those of sulfur in all the cases. In comparison with the model fuel #1, lack of nitrogen containing compounds in the model fuel #2 results in an increase of about 15.28%, 14.54%, and 16.42% in sulfur adsorption for MSU-S, HPW-MSU-S, and Ni/HPW-MSU-S respectively; however, using the model fuel #3 without any sulfur species shows only less than 3% more nitrogen adsorbing compared to the model fuel #1 for all the three adsorbents. The sulfur selectivities of MSU-S, HPW-MSU-S, and Ni/HPW-MSU-S in the adsorption with the model fuel #1 (0.4443, 0.4782, and 0.4991 respectively) indicate that all the three adsorbents slightly prefer nitrogen to sulfur adsorption. Moreover, the addition of phosphotungstic acid (HPW) and Ni-HPW to MSU-S increases the adsorption loadings of sulfur species from the model fuel #1 by21.6% and 33.2% respectively. For nitrogen adsorption with the model fuel #1, loading increases of 6.1% and 6.9% occurs in HPW and Ni-HPW modified adsorbents respectively; however, the textural specifications of MSU-S decrease with the loading of Ni and HPW. Considering the acidity of the adsorbents can explain this opposition. In spite of decreasing specific surface area, the surface acidity of adsorbent increases much more in the presence of HPW and nickel, which consequently leads to an increase in the adsorption of sulfur and nitrogen compounds. The loading of HPW and nickel on adsorbent has drastic effects on desulfurization process in spite of its negligible impact on nitrogen removal performance. In other words, increasing the acidic properties of adsorbents with either HPW or Ni species plays an important role in sulfur adsorption over MSU-S. The inhibiting effect of the nitrogen-containing compounds on desulfurization is much stronger than the effect of the sulfurous species on denitrogenation. This indicates that nitrogen compounds are obviously the predominant side in adsorption and sulfur compounds have to compete with them to occupy more active sites.

Table 2
Adsorption loading and capacity of the three adsorbents for total sulfur and total nitrogen.

Adsorbent	Model Fuel #1					Model Fuel #2		Model Fuel #3	
	q_S	Q_S	q_N	Q_N	Sulfur Selectivity	q_S	Q_S	q_N	Q_N
MSU	0.3273	0.0154	0.4093	0.0084	0.4443	0.3773	0.0178	0.4172	0.0086
HPW-MSU	0.3979	0.0196	0.4341	0.0093	0.4782	0.4558	0.0225	0.4442	0.0095
Ni/HPW-MSU	0.4359	0.0397	0.4374	0.0174	0.4991	0.5075	0.0463	0.4471	0.0178

3.3. Adsorption kinetic

More than 90% of adsorption loading at equilibrium state over MSU-S is attained during first 50 min contact time for nitrogen and sulfur contents. By using HPW, the time for reaching at least 90% of equilibrium adsorption loading is reduced to 40 minutes for all the species. The adsorption loading was reached to more than 90% of its equilibrium value up to the 30th minute of contact time for all the nitrogen and sulfur compounds over Ni/HPW-MSU-S. This indicates that Ni-HPW loading can reduce the time for reaching adsorption equilibrium more than pure HPW. Three more widely used kinetic models were examined for best fitting the adsorption results. After integration, the pseudo first-order Lagergren model turns to the form of:

$$\ln(q_e - q_t) = \ln q_e - k_f t \tag{5}$$

The integrated form of pseudo second-order model is given as:

$$t/q_t = 1/k_s {q_e}^2 + t/q_e \tag{6}$$

The intraparticle diffusion Weber and Morris model is expressed in the form of:

$$q_t = k_i t^{1/2} + C \tag{7}$$

In the above equations, q_e and q_t are the adsorption uptake of a component or element per the unit mass of the adsorbent in equilibrium and in time period of t ($mg.g^{-1}$) respectively; k_f, k_s, and k_i represent the rate constant of pseudo-first order (min^{-1}), pseudo-second order ($g.mg^{-1}.min^{-1}$), and intraparticle diffusion ($mg.g^{-1}.min^{-0.5}$) respectively. C is a constant ($mg.g^{-1}$). Using the experimental results and data regression of Equations 5-7, q_e, k_f, k_s, k_i, and C can be determined from the plot slop and interception of the equations as given in Tables 3. As obviously can be seen, the pseudo-second order model with the highest correlation coefficients ($0.995<R^2<0.999$) presents the best fitting of adsorption data for both nitrogen and sulfur over each adsorbent compared to the pseudo-first order model ($0.483<R^2<0.917$) and intraparticle diffusion model ($0.588<R^2<0.739$). The poor fitting of the experimental data in the case of intraparticle diffusion model indicates that the diffusion process may be controlled by more than one step (Wen et al., 2010; Xu et al., 2013). The adsorption of total nitrogen occurs much faster than that of the total sulfur for all the samples.

Table 3
Kinetic analysis results of the three adsorbents.

Adsorbent	Species	Pseudo First-order			Pseudo Second-order			Intraparticle Diffusion		
		$q_{e,cal}$	k_f	R^2	$q_{e,cal}$	k_s	R^2	C	k_i	R^2
MSU	**N**	2.671	0.028	0.917	6.006	0.019	0.995	2.815	0.437	0.708
	S	4.746	0.021	0.888	10.822	0.011	0.997	5.849	1.139	0.739
HPW-MSU	**N**	2.262	0.025	0.917	6.234	0.031	0.998	3.113	0.436	0.667
	S	4.054	0.024	0.862	13.106	0.013	0.997	9.045	1.123	0.619
Ni/HPW-MSU	**N**	6.882	0.058	0.537	6.257	0.042	0.998	3.376	0.445	0.619
	S	11.572	0.046	0.483	14.064	0.024	0.999	11.075	1.331	0.588

3.4. Adsorption equilibrium

Freundlich and Langmuir isotherms were used to analyze the adsorption data using the model fuel #1 with different initial contents of sulfur/nitrogen (S/N) species. The linear forms of the equations are given by:

Langmuir:

$$1/q = 1/q_m + (1/K_L\, q_m C_s) \tag{8}$$

Freundlich:

$$\ln q = \ln K_F + (1/n) \ln C_s \tag{9}$$

where, K_L (kg.mg^{-1}) and q_m (mg.g^{-1}) are the Langmuir constants related to the energy of adsorption and maximum loading respectively; K_F (mg$^{1-(1/n)}$.g^{-1}.kg$^{1/n}$) and $1/n$ represent Freundlich constants related to the adsorption capacity and adsorption intensity respectively; C_s (mg.kg^{-1}) and q (mg.g^{-1}) stand for the concentration and adsorption loading of sulfur/nitrogen (S/N) at equilibrium respectively. The regression of the experimental data allows us to find K_L and q_m for Equation 8, and also K_F and $1/n$ in Equation 9 from the slope and interception of the plotted equations. The mentioned parameters along with the correlation coefficient R^2 values of the two models were given in Table 4 for each adsorbent.

Table 4
Isotherm analysis results of the three adsorbents.

Adsorbent	Species	Langmuir			Freundlich		
		q_m	K_L	R^2	$1/n$	K_F	R^2
MSU	**N**	5.420	3.624	0.997	0.192	2.277	0.974
	S	14.409	1.031	0.986	0.194	4.051	0.968
HPW-MSU	**N**	5.747	6.718	0.997	0.184	2.532	0.977
	S	10.493	1.961	0.967	0.196	3.183	0.985
Ni/HPW-MSU	**N**	5.414	18.107	0.985	0.165	2.676	0.996
	S	11.821	5.834	0.961	0.163	4.449	0.978

Data fitting for total nitrogen is achieved better by the Langmuir model than Freundlich model for MSU-S and HPW-MSU-S (R^2 value of 0.997). Langmuir model also describes the adsorption of total sulfur over MSU-S better than the other model does with R^2 value of 0.986. Langmuir model is the best one for homogeneous adsorption process with finite monolayer coverage of adsorbates on the sorbent surface, leading to a fixed maximum loading (q_m) at high concentrations (Okeola et al., 2010; Wen et al., 2010; Desta, 2013; Xu et al., 2013). The q_m value of nitrogen is lower than that of sulfur over MSU-S, which may be due to the larger molecular dimensions of nitrogen compounds in comparison to that of sulfur ones. The larger K_L value belongs to nitrogen when HPW-impregnated adsorbent is employed, indicating the greater affinity of active sites for nitrogen than sulfur (Okeola et al., 2010; Li et al., 2011; Desta, 2013). Adsorption affinity has been quantified by a separation factor or equilibrium parameter (R_L); it determines the type of Langmuir isotherm as irreversible ($R_L = 0$), linear ($R_L = 1$), unfavorable ($R_L > 1$), or favorable ($0 < R_L < 1$) (Desta, 2013).

$$R_L = 1/(1 + K_L C_S) \tag{10}$$

This factor is in the range of 0-1 for all the cases, indicating the favorable type of all the Langmuir adsorptions. It can be seen that the data of total sulfur are fitted very well to the Freundlich model with R^2 values of 0.985 for HPW-MSU-S. This indicates that sulfur adsorption over HPW-MSU-S is heterogeneous and infinite surface coverage of the adsorbates is occurred without maximum adsorption, which may be considered as a multilayer adsorption (Dehkordi et al., 2009; Wen et al., 2010; Arcibar-Orozco et al., 2013). Freundlich model can also fit the adsorption data of all the species over Ni/HPW-MSU-S better than Langmuir model ($0.978<R^2<0.996$). Depending on n value, adsorption process may be linear ($1/n=1$), chemical ($1/n>1$), or physical ($1/n<1$), indicating the nonlinearity degree of adsorption. Therefore, all the species are adsorbed on three sorbents through a physical process as a result of decreasing adsorbent-adsorbate interaction with increasing surface density (Okeola et al., 2010; Desta, 2013). Similar to q_m, the value of K_F shows the adsorption performance (Okeola et al., 2010). The greatest and lowest value of K_F, i.e. 4.449 and 2.676, belongs to sulfur and nitrogen respectively for Ni/HPW-MSU-S.

Generally, the obtained adsorption capacities are better than previous works (Santos et al., 2012; Sarda et al., 2012; Shahadat Hussain et al., 2013; Teymouri et al., 2013) for sulfur removal. The comparison of some adsorbents utilized through batch tests for desulfurization and denitrogenation is mentioned in more details in Table 5. Although activated carbon adsorption capacity for nitrogen compound removal is more than the present work, this adsorbent is not as good as Ni/HPW-MSU-S. In other words, the present novel adsorbent has the ability to remove both sulfur and nitrogen compounds simultaneously.

Table 5
Comparison of textural properties and S/N adsorption capacity of different adsorbents.

Adsorbent	Specific Surface Area (m^2/g)	Pore Volume (cm^3/g)	Sulfur Adsorption (mmol S/g A)	Nitrogen Adsorption (mmol N/g A)
AC (pet. coke source)[a]	1036	-	-	0.89
10% Ni/Al_2O_3[b]	140	-	0.013	-
$Mo/Al_2O_3–SiO_2$[c]	275	0.59	0.039	0.13
$Ce/Al_2O_3–SiO_2$[c]	217	0.43	0.031	0.09
$Ni/Al_2O_3–SiO_2$[c]	292	0.42	0.037	0.12
4% $Ag/TiO_x–Al_2O_3$[d]	222	0.61	0.33	-
Present work: Ni/HPW-MSU-S	351.3	0.68	0.435	0.438

a: Li et al., 2011
b: Sarda et al., 2012
c: Santos et al., 2012
d: Shahadat Hussain et al., 2013

4. Conclusions

The performance of MSU-S and its modified forms with phosphotungstic acid and nickel for the desulfurization and denitrogenation of the model diesel fuels were studied at room temperature in a batch process. Quinoline, carbazole, thiophene, and dibenzothiophene were selected as the model compounds in the fuels. According to the results of the characteristic tests (N_2 adsorption-desorption, XRD, SEM, and NH_3-TPD), heteropoly acid incorporation causes a higher acidity along with a negligible loss in the structural aspects, while Ni impregnation leaves two significant effects on MSU-S, namely a negative effect on mesoporous structure, crystalline phase, and particle shape along with a positive impact on surface acidity; also, the positive effect outweighs the negative one and consequently results in an improvement in S/N adsorption compared to MSU-S and HPW-MSU-S. With both of HPW and Ni modifications, the maximum increase of 33.18% and 6.88% is respectively occurred for the adsorption loading of total sulfur and total nitrogen from the first model fuel. The best result in the desulfurization of the first model fuel is 22.51%, corresponding to the adsorption loading of 0.435 mmol/g and adsorption capacity of 0.039 mg/m^2. The best corresponding efficiency of nitrogen removal is 45.13% with an adsorption loading and capacity of 0.438 mmol/g and 0.018 mg/m^2 respectively. The adsorption loading and selectivity of all the adsorbents for total nitrogen were slightly more than those for total sulfur, which represents the selective adsorption of nitrogen over sulfur. The Ni-HPW loaded adsorbent has the greatest adsorption selectivity for sulfur compared to the others, indicating a direct relationship between metal/acid loading and adsorption selectivity for sulfur. According to the best fit of Freundlich model with equilibrium isotherms of adsorption using Ni/HPW-MSU-S, it is obviously concluded that adsorption on the surface of Ni-HPW loaded MSU-S is heterogeneous. The kinetic results introduce the pseudo-second order model as the best one for fitting the adsorption data of all the species over each adsorbent. The adsorption rate of total nitrogen is about 2 times higher than that of total sulfur.

For improving the results, several options such as use of different metals, employing other impregnation methods, displacement of HPW, metal interchangeably, etc. are suggested. As supplementary researches, regeneration ability, fixed-bed adsorption, and other types of fuel such as gasoline can be investigated in the future works. For the adsorptive removal of nitrogen and sulfur from fuels, it is better to apply such compounds to the output streams of refineries or before consumption sectors.

5. Acknowledgments

The authors would like to thank the Petroleum University of Technology for financially supporting this study.

Nomenclature

AC	: Activated carbon
BET	: Brauner Emmett Teller
BJH	: Barrett Joyner Halenda
DBT	: Dibenzothiophene
FID	: Flame ionization detector
GC	: Gas chromatograph
HDN	: Hydrodenitrogenation
HDS	: Hydrodesulfurization
HPW	: Phosphotungstic acid (H3PW12O40)
HTABr	: Hexadecyltrimethylammonium bromide
MFI	: Mobil-5
MSU	: Michigan State University
ODN	: Oxidative denitrogenation
ODS	: Oxidative desulfurization
SEM	: Scanning electron microscopy
TCD	: Thermal conductivity detector
TN	: Total nitrogen
TPAOH	: Tetrapropylammonium hydroxide
TPD	: Temperature programmed desorption
TS	: Total sulfur
XRD	: X-ray diffraction

References

Arcibar-Orozco, J. A. and Rangel-Mendez, J. R., Model Diesel Denitrogenation by Modified Activated Carbon with Iron Nanoparticles: Sulfur Compound Effect, Chemical Engineering Journal, Vol. 230, p. 439-446, 2013.

Bernstein, J. A., Alexis, N., Bacchus, H., Bernstein, I. L., Fritz, P., Horner, E., Li, N., Mason, S., Nel, A., Oullette, J., Reijula, K., Reponen, T., Seltzer, J., Smith, A., and Tarlo, S. M., The Health Effects of Nonindustrial Indoor Air Pollution, Journal of Allergy and Clinical Immunology, Vol. 121, No. 3, p. 585-591, 2008.

Chen, H., Wang, Y., Yang, F. H., and Yang, R. T., Desulfurization of High-sulfur Jet Fuel by Mesoporous π-complexation Adsorbents, Chemical Engineering Science, Vol. 64, No. 24, p. 5240-5246, 2009.

Dehkordi, A. M., Kiaei, Z., and Sobati, M. A., Oxidative Desulfurization of Simulated Light Fuel Oil and Untreated Kerosene, Fuel Processing Technology, Vol. 90, No. 3, p. 435-445, 2009.

Desta, M. B., Batch Sorption Experiments: Langmuir and Freundlich Isotherm Studies for the Adsorption of Textile Metal Ions onto Teff Straw (Eragrostis Tef) Agricultural Waste, Journal of Thermodynamics, Vol. 2013, p. 1-6, 2013.

Erisman, J. W., Bleeker, A., Galloway, J., and Sutton, M. S., Reduced Nitrogen in Ecology and the Environment, Environmental Pollution, Vol. 150, No. 1, p. 140-149, 2007.

Gagea, B. C., Lorgouilloux, Y., Altintas, Y., Jacobs, P. A., and Martens, J. A., Bifunctional Conversion of n-Decane over HPW Heteropoly Acid Incorporated into SBA-15 during Synthesis, Journal of Catalysis, Vol. 265, No. 1, p. 99-108, 2009.

Kampa, M. and Castanas, E., Human Health Effects of Air Pollution, Environmental Pollution, Vol. 151, No. 2, p. 362-367, 2008.

Kim, J. H., Ma, X., Zhou, A., and Song, C., Ultra-deep Desulfurization and Denitrogenation of Diesel Fuel by Selective Adsorption over Three Different Adsorbents: A Study on Adsorptive Selectivity and Mechanism, Catalysis Today, Vol. 111, No. 1-2, p. 74-83, 2006.

Koriakin, A., Ponvel, K. M., and Lee, C.-H., Denitrogenation of Raw Diesel Fuel by Lithium-modified Mesoporous Silica, Chemical Engineering Journal, Vol. 162, No. 2, p. 649-655, 2010.

Kraft, M., Eikmann, T., Kappos, A., Künzli, N., Rapp, R., Schneider, K., Seitz, H., Voss, J.-U., and Wichmann, H. E., The German View: Effects of Nitrogen Dioxide on Human Health–derivation of Health-related Short-term and Long-term Values, International Journal of Hygiene and Environmental Health, Vol. 208, No. 4, p. 305-318, 2005.

Kugita, T., Jana, S. K., Owada, T., Hashimoto, N., Onaka, M., and Namba, S., Mesoporous Al-Containing MCM-41 Molecular Sieves: Highly Active Catalysts for Diels–Alder Reaction of Cyclopentadiene with α,β-unsaturated Aldehydes, Applied Catalysis A: General, Vol. 245, No. 2, p. 353-362, 2003.

Latza, U., Gerdes, S., and Baur, X., Effects of Nitrogen Dioxide on Human Health: Systematic Review of Experimental and Epidemiological Studies Conducted between 2002 and 2006, International Journal of Hygiene and Environmental Health, Vol. 212, No. 3, p. 271-287, 2009.

Li, N., Almarri, M., Ma, X. l., and Zha, Q. f., The Role of Surface Oxygen-containing Functional Groups in Liquid-phase Adsorptive Denitrogenation by Activated Carbon, New Carbon Materials, Vol. 26, No. 6, p. 470-478, 2011.

Liu, Y., Zhang, W., and Pinnavaia, T. J., Steam-Stable MSU-S Aluminosilicate Mesostructures Assembled from Zeolite ZSM-5 and Zeolite Beta Seeds, Angewandte Chemie International Edition, Vol. 40, No. 7, p. 1255-1258, 2001.

Lourenço, J. P., Fernandes, A., Henriques, C., and Ribeiro, M. F., Al-containing MCM-41 Type Materials Prepared by Different Synthesis Methods: Hydrothermal Stability and Catalytic Properties, Microporous and Mesoporous Materials, Vol. 94, No. 1-3, p. 56-65, 2006.

Meng, C., Fang, Y., Jin, L., and Hu, H., Deep Desulfurization of Model Gasoline by Selective Adsorption on Ag+/Al-MSU-S, Catalysis Today, Vol. 149, No. 1-2, p. 138-142, 2010.

Naik, S. P., Bui, V., Ryu, T., Miller, J. D., and Zmierczak, W., Al-MCM-41 As Methanol Dehydration Catalyst, Applied Catalysis A: General, Vol. 381, No. 1-2, p. 183-190, 2010.

Okeola, F. O. and Odebunmi, E. O., Freundlich and Langmuir Isotherms Parameters for Adsorption of Methylene Blue by Activated Carbon Derived from Agrowastes, Advances in Natural and Applied Sciences, Vol. 4, No. 3, p. 281-288, 2010.

Pan, X., Sulfur Oxides: Sources, Exposures and Health Effects, Encyclopedia of Environmental Health, Nriagu, J. O., Burlington, Elsevier, p. 290-296, 2011.

Rouquerol, J., Avnir, D., Fairbridge, C., Everett, D., Haynes, J., Pernicone, N., Ramsay, J., Sing, K., and Unger, K., Recommendations for the Characterization of Porous Solids (Technical Report), Pure and Applied Chemistry, Vol. 66, No. 8, p. 1739-1758, 1994.

Santos, A. L., Reis, R. A., Rossa, V., Reis, M. M., Costa, A. L. H., Veloso, C. O., Henriques, C. A., Zotin, F. M. Z., Paredes, M. L. L., Silveira, E. B., and Chiaro, S. S. X., Silica–alumina Impregnated with Cerium, Nickel, and Molybdenum Oxides for Adsorption of Sulfur and Nitrogen Compounds from Diesel, Materials Letters, Vol. 83, p. 158-160, 2012.

Sarda, K. K., Bhandari, A., Pant, K. K., and Jain, S., Deep Desulfurization of Diesel Fuel by Selective Adsorption over Ni/Al2O3 and Ni/ZSM-5 Extrudates, Fuel, Vol. 93, p. 86-91, 2012.

Shahadat Hussain, A. H. M. and Tatarchuk, B. J., Adsorptive Desulfurization of Jet and Diesel Fuels using Ag/TiOx–Al2O3 and Ag/TiOx–SiO2 Adsorbents, Fuel, Vol. 107, p. 465-473, 2013.

Sing, K. S. W., Reporting Physisorption Data for Gas/solid Systems with Special Reference to the Determination of Surface Area and Porosity (Recommendations 1984), Pure and Applied Chemistry, Vol. 57, No. 4, p. 603-619, 1985.

Sun, B., Li, G. and Wang, X., Facile Synthesis of Microporous Carbon through a Soft-template Pathway and its Performance in Desulfurization and Denitrogenation, Journal of Natural Gas Chemistry, Vol. 19, No. 5, p. 471-476, 2010.

Teymouri, M., Samadi-Maybodi, A., Vahid, A., and Miranbeigi, A., Adsorptive Desulfurization of Low Sulfur Diesel Fuel Using Palladium Containing Mesoporous Silica Synthesized via a Novel in-situ Approach, Fuel Processing Technology, Vol. 116, p. 257-264, 2013.

Wang, J., Hua, W., Yue, Y., and Gao, Z., MSU-S Mesoporous Materials: An Efficient Catalyst for Isomerization of α-pinene, Bioresource Technology, Vol. 101, No. 19, p. 7224-7230, 2010.

Wang, L., Sun, B., Yang, F. H., and Yang, R. T., Effects of Aromatics on Desulfurization of Liquid Fuel by π-complexation and Carbon Adsorbents, Chemical Engineering Science, Vol. 73, p. 208-217, 2012.

Wen, J., Han, X., Lin, H., Zheng, Y., and Chu, W., A Critical Study on the Adsorption of Heterocyclic Sulfur and Nitrogen Compounds by Activated Carbon: Equilibrium, Kinetics and Thermodynamics, Chemical Engineering Journal, Vol. 164, No. 1, p. 29-36, 2010.

Xu, X., Zhang, S., Li, P., and Shen, Y., Equilibrium and Kinetics of Jet-A Fuel Desulfurization by Selective Adsorption at Room Temperatures, Fuel, Vol. 111, p. 172-179, 2013.

Xu, X., Zhang, S., Li, P., and Shen, Y., Desulfurization of Jet-A Fuel in a Fixed-bed Reactor at Room Temperature and Ambient Pressure Using a Novel Selective Adsorbent, Fuel, Vol. 117, p. 499-508, 2014.

Yang, L., Wang, S., Wang, R., and Yu, H., Selective Removal of Nitrogen-containing Heterocyclic Compounds from Transportation Diesel Fuels with Reactive Adsorbent, Chinese Journal of Chemical Engineering, Vol. 21, No. 5, p. 558-563, 2013.